

The Influence of the Optical Phonons on the Non-equilibrium Spin Current in the Presence of Spin–Orbit Couplings

K. Hasanirokh¹ · A. Phirouznia¹ · R. Majidi²

Received: 15 March 2015 / Accepted: 6 December 2015 / Published online: 28 December 2015
© Springer Science+Business Media New York 2015

Abstract The influence of the electron coupling with non-polarized optical phonons on magnetoelectric effects of a two-dimensional electron gas system has been investigated in the presence of the Rashba and Dresselhaus spin–orbit couplings. Numerical calculations have been performed in the non-equilibrium regime. In the previous studies in this field, it has been shown that the Rashba and Dresselhaus couplings cannot generate non-equilibrium spin current and the spin current vanishes identically in the absence of other relaxation mechanisms such as lattice vibrations. However, in the current study, based on a semiclassical approach, it was demonstrated that in the presence of electron–phonon coupling, the spin current and other magnetoelectric quantities have been modulated by the strength of the spin–orbit interactions.

1 Introduction

During the last several years, spin-based semiconductor electronics has attracted more attention that the electron spin rather than electron charge is at the very center attention [1, 2].

The pure spin current is a flow of particles with opposite spin projections in opposite directions. The generation and effective control of the spin-polarized currents are necessary and very important for the practical implementation of semiconducting spin electronics. Many device setups, based on the spin–orbit interactions (SOIs),

✉ K. Hasanirokh
zhasanirokh@yahoo.com

A. Phirouznia
phirouznia@azaruniv.ac.ir

¹ Physics Department, Azarbaijan Shahid Madani University, Tabriz, Iran

² Department of Physics, Shahid Rajaee University, Tehran, Iran

have been proposed to produce a spin-polarized transport current in semiconductors [3]. The Rashba SOI is a prime instance which arises due to the presence of structure inversion asymmetry (SIA) introduced by heterojunction surfaces or external fields [4]. This type of SOI led Datta and Das to design a spin field-effect transistor (SFET) [5–7], in which the spin of the electron passing the device is controlled by the Rashba SOI. In the presence of structure inversion asymmetry, the proposed transistor has generated great attention in the field of mesoscopic spin-polarized transport.

The other spin-orbit coupling that occurs in structures without the bulk inversion asymmetry [8] is the Dresselhaus coupling [9]. These two different SOIs introduce an effective magnetic field that can effectively control both the magnitude and direction of non-equilibrium spin accumulation [10].

By forgoing SOIs and short-range delta function impurity, Huang and Hu found the accountable spin accumulation; however, they have shown that the spin current vanishes identically in the non-equilibrium regime in a two-dimensional electron gas [10]. In addition, based on the Green’s function approach, Inoue obtained a similar conclusion for two-dimensional electron gas structures [11].

It should be noted that for the Rashba type two-band model, the discrepancy between the exact method and approximative Boltzmann approach ($1/\tau$ approach) remains only on the higher order corrections [12, 13].

In this work, based on the semiclassical approach, we have theoretically investigated the spin-transport quantities in a two-dimensional electron gas when the spin-orbit couplings, magnetic impurity, and optical phonon scattering are present. Electron-phonon scattering leads to the non-vanishing spin current that can be controlled by the strength of spin-orbit interactions. Results have also shown that spin accumulation and spin torque are critically dependent on the deformation potential and the Rashba coupling constant.

2 Model and Approach

In the presence of lattice vibrations of a two-dimensional electron gas can be described by the following Hamiltonian $\hat{H} = \hat{H}_0 + \hat{H}_{el-ph} + V_{im}$. Here \hat{H}_0 is the kinetic energy and spin-orbit Hamiltonian including both of the Rashba and Dresselhaus spin-orbit couplings that in the basis of plane waves functions is given as follows [4, 9]:

$$\hat{H}_0 = \frac{\hbar^2 k^2}{2m} + \alpha(\hat{\sigma}_x k_y - \hat{\sigma}_y k_x) + \beta(\hat{\sigma}_x k_x - \hat{\sigma}_y k_y), \tag{1}$$

in which \mathbf{k} represents the wave vector of conduction electrons, $\sigma_i (i = x, y)$ are Pauli matrices, α and β denote the Rashba and Dresselhaus strengths, respectively. For a given wave vector \mathbf{k} , the eigenfunctions of \hat{H}_0 are determined as

$$|\mathbf{k}\lambda\rangle = \frac{1}{\sqrt{2}} \begin{pmatrix} e^{i\frac{\phi_{\mathbf{k}}}{2}} \\ \lambda e^{-i\frac{\phi_{\mathbf{k}}}{2}} \end{pmatrix}, \tag{2}$$

where $\lambda = \pm 1$ and the angle $\phi_{\mathbf{k}}$ are defined easily by

$$\tan \phi_{\mathbf{k}} = \frac{\alpha k_x + \beta k_y}{\alpha k_y + \beta k_x}. \tag{3}$$

The corresponding eigenvalues of \hat{H}_0 are $\epsilon_{\mathbf{k}\lambda} = \lambda \sqrt{(\alpha^2 + \beta^2)k^2 + 4\alpha\beta k_x k_y}$. The expectation values of the electron spin along the x and y directions in the state $|\mathbf{k}\lambda\rangle$ can be found to be

$$S_{\lambda,x}^{(0)}(\mathbf{k}) = \frac{\hbar}{2}\lambda \cos(\phi_{\mathbf{k}}), \quad S_{\lambda,y}^{(0)}(\mathbf{k}) = \frac{-\hbar}{2}\lambda \sin(\phi_{\mathbf{k}}). \tag{4}$$

The second term of the total Hamiltonian, \hat{H}_{el-ph} , is the electron–phonon interaction that can be expressed as [14]

$$\hat{H}_{el-ph} = D_{opt} \cdot U(\vec{r}). \tag{5}$$

D_{opt} is the deformation potential for electron scattering by optical phonons and $U(\vec{r})$ is defined as displacement vector of an ion from equilibrium position \vec{R} . For the two-dimensional system, the displacement vector is determined as

$$U(\vec{r}) = \sum_q \sqrt{\frac{\hbar}{2MNW_e}} \vec{e}_q [a_q e^{i\vec{q}\cdot\vec{r}} + a_q^\dagger e^{-i\vec{q}\cdot\vec{r}}], \tag{6}$$

where N and M are number of the ions and ion mass, respectively. \vec{e}_q is the unit vector in displacement direction and a_q^\dagger/a_q are the creation/annihilation operators for phonons with wave vector q .

Therefore, we obtain directly the following result:

$$\hat{H}_{el-ph} = \sum_q [C(q)a_q e^{i\vec{q}\cdot\vec{r}} + C^*(q)a_q^\dagger e^{-i\vec{q}\cdot\vec{r}}]. \tag{7}$$

where

$$C(q) = D_{opt} \sqrt{\frac{\hbar}{2MNW_e}} (i\hat{e}_q \cdot \vec{q}). \tag{8}$$

The eigenstate of the electron–phonon Hamiltonian in harmonic approximation is defined by $|n\rangle$, where n is the Bose–Einstein distribution function of phonons, so we can define a new basis as follows, $|\mathbf{k}\lambda n\rangle = |\mathbf{k}\lambda\rangle \otimes |n\rangle$. The scattering matrix of electron–phonon interaction is given by

$$\langle \mathbf{k}'\lambda'n'_q | \hat{H}_{el-ph} | \mathbf{k}\lambda n_q \rangle = \begin{cases} \delta_{n'_q, n_q-1} \delta_{\lambda'\lambda} C(q) \sqrt{n_q}, & \text{if } \mathbf{k}' = \mathbf{k} + \mathbf{q}, \\ \delta_{n'_q, n_q+1} \delta_{\lambda'\lambda} C^*(q) \sqrt{n_q + 1}, & \text{if } \mathbf{k}' = \mathbf{k} - \mathbf{q}. \end{cases} \tag{9}$$

The last term of the total Hamiltonian, $V_{im}(r)$, is the impurity scattering potential that can be defined by

$$V_{im}(r) = \sum_i J \hat{\sigma} \cdot \vec{m} \delta(\mathbf{r} - \mathbf{r}_i), \tag{10}$$

where J is the exchange interaction constant of magnetic impurities with conduction electrons and \hat{m} denotes the unit vector of the magnetization.

$$\langle \mathbf{k}'\lambda'n'_q | V_{im}(r) | \mathbf{k}\lambda n_q \rangle = \delta_{\hat{n}_q, n_q} \delta_{\hat{\mathbf{k}}, \mathbf{k}} \begin{pmatrix} J_z & J_x + iJ_y \\ J_x + iJ_y & -J_z \end{pmatrix}. \tag{11}$$

Here $J_z = \hat{m}_z J$, $J_y = \hat{m}_y J$, $J_x = \hat{m}_x J$. For long-range magnetic interactions, due to the shape anisotropy, we take $\hat{m}_z = 0$ and because of the random distribution, we assume $\langle m_x \rangle = \langle m_y \rangle = 0$ that $\langle m_x^2 \rangle = \langle m_y^2 \rangle = \frac{1}{2}$. We have also used the approximation $\sum_j \exp(i\vec{q} \cdot \vec{r}_j) \simeq 1$ and $\sum_j \sum_{j'} \exp(i\vec{q} \cdot (\vec{r}_j - \vec{r}_{j'})) = n_i$, where n_i is the impurity density.

For spin-dependent and spin-independent relaxation mechanisms, we have considered the two last terms of the total Hamiltonian, so we can rewrite these two terms as

$$V = \hat{V}_{im} + \hat{H}_{el-ph} \tag{12}$$

The scattering state of a conduction electron is determined from the Lippman-Schwinger equation where in the Born approximation one has

$$| \mathbf{k}\lambda n_q \rangle_{scat} = | \mathbf{k}\lambda n_q \rangle + \sum_{\mathbf{k}'\lambda'\eta} \frac{V_{\mathbf{k}'\lambda'\eta, \mathbf{k}\lambda n_q}}{\epsilon_{\mathbf{k}\lambda} - \epsilon_{\mathbf{k}'\lambda'} + i\eta} | \mathbf{k}'\lambda'\eta \rangle, \tag{13}$$

where η is a small positive quantity. Then the expectation value of the electron spin is modified as follows:

$$S_{\lambda,i}(\mathbf{k}) = S_{\lambda,i}^{(0)}(\mathbf{k}) + \hbar \sum_{\mathbf{k}'\lambda'\eta} Re \left[\frac{V_{\mathbf{k}'\lambda'\eta, \mathbf{k}\lambda n_q} \langle \sigma_i \rangle_{\mathbf{k}'\lambda'\eta, \mathbf{k}\lambda n_q}}{\epsilon_{\mathbf{k}\lambda} - \epsilon_{\mathbf{k}'\lambda'} + i\eta} \right], \tag{14}$$

where we have defined $S_{\lambda,i}(\mathbf{k}) = \langle \mathbf{k}\lambda n | \hat{S}_i | \mathbf{k}\lambda n \rangle_{scat}$. One can write

$$S_{\lambda,i}(\mathbf{k}) = S_{\lambda,i}^{(0)}(\mathbf{k}) + \hbar \sum_{\mathbf{k}'\lambda'} Re \left[V_{\mathbf{k}'\lambda', \mathbf{k}\lambda n} \langle \hat{\sigma}_i \rangle_{\mathbf{k}'\lambda', \mathbf{k}\lambda n} Pr \frac{1}{\epsilon_{\mathbf{k}\lambda} - \epsilon_{\mathbf{k}'\lambda'}} - V_{\mathbf{k}'\lambda', \mathbf{k}\lambda n} \langle \sigma_i \rangle_{\mathbf{k}'\lambda', \mathbf{k}\lambda n} i\pi \delta(\epsilon_{\mathbf{k}\lambda} - \epsilon_{\mathbf{k}'\lambda'}) \right], \tag{15}$$

where $\langle \sigma_i \rangle_{\mathbf{k}'\lambda', \mathbf{k}\lambda n}$ is the expectation value of the Pauli Matrix in a Lippman-Schwinger scattering state. The i th component of the net spin density can be given

by

$$\langle S_i \rangle = \sum_{\lambda, \mathbf{k}, \mathbf{q}} S_{\lambda, i}(\mathbf{k}) f_{\lambda}(\mathbf{k}, \mathbf{q}), \tag{16}$$

where $f_{\lambda}(\mathbf{k}, \mathbf{q})$ is the distribution function of conduction electrons, and in the absence of external electric field, it will be given by the equilibrium Fermi distribution function,

$$f_{\lambda}(\mathbf{k}, \mathbf{q}) = f_0(\epsilon_{\mathbf{k}\lambda}) = \frac{1}{1 + e^{\frac{(\epsilon_{\mathbf{k}\lambda} - \epsilon_F)}{k_B T}}}. \tag{17}$$

To drive the non-equilibrium distribution function for a homogeneous system, we solve the Boltzmann transport equation for a steady state (in the weak scattering regime),

$$\dot{\mathbf{k}} \cdot \frac{\partial f_{\lambda}(\mathbf{k})}{\partial \mathbf{k}} = \left(\frac{\partial f_{\lambda}}{\partial t} \right)_{coll}, \tag{18}$$

in which $\dot{\mathbf{k}} = \frac{-e\mathbf{E}}{\hbar}$ and the collision integral due to scatterings, $\left(\frac{\partial f_{\lambda}}{\partial t} \right)_{coll}$, reads [15]

$$\begin{aligned} \left(\frac{\partial f_{\lambda}}{\partial t} \right) = & - \sum_{\mathbf{k}'\mathbf{q}'\lambda'} W_{\mathbf{k}'\lambda'\hat{n},\mathbf{k}\lambda n} f_{\lambda}(\mathbf{k})(1 - f_{\lambda'}(\mathbf{k}')\delta(\epsilon_{\mathbf{k}\lambda} - \epsilon_{\mathbf{k}'\lambda'})) + \\ & \sum_{\mathbf{k}'\mathbf{q}'\lambda'} W_{\mathbf{k}'\lambda'\hat{n},\mathbf{k}\lambda n} f_{\lambda'}(\mathbf{k}')(1 - f_{\lambda}(\mathbf{k}))\delta(\epsilon_{\mathbf{k}\lambda} - \epsilon_{\mathbf{k}'\lambda'}) + \\ & \sum_{\mathbf{k}'\mathbf{q}'\lambda'} W_{\mathbf{k}'\lambda'\hat{n},\mathbf{k}\lambda n}^{(2)} (f_{\lambda'}(\mathbf{k}-\mathbf{q}) - f_{\lambda}(\mathbf{k}))\delta(\epsilon_{\mathbf{k}'\lambda'} - \epsilon_{\mathbf{k}\lambda} - \hbar\omega)\delta(\mathbf{k}' - \mathbf{k} - \mathbf{q}) + \\ & \sum_{\mathbf{k}'\mathbf{q}'\lambda'} W_{\mathbf{k}'\lambda'\hat{n},\mathbf{k}\lambda n}^{(3)} (f_{\lambda'}(\mathbf{k}+\mathbf{q}) - f_{\lambda}(\mathbf{k}))\delta(\epsilon_{\mathbf{k}'\lambda'} - \epsilon_{\mathbf{k}\lambda} + \hbar\omega)\delta(\mathbf{k}' - \mathbf{k} + \mathbf{q}) \end{aligned} \tag{19}$$

$W_{\mathbf{k}'\lambda'\hat{n},\mathbf{k}\lambda n}$ are the transition probabilities which are given by Fermi's golden rule, $W_{\mathbf{k}'\lambda'\hat{n},\mathbf{k}\lambda n} = \frac{2\pi}{\hbar} |V_{\mathbf{k}'\lambda'\hat{n},\mathbf{k}\lambda n}|^2$.

$\delta_{\hat{n},n}\delta_{\hat{\mathbf{k}},\mathbf{k}}$ selects the diagonal elements of $|V_{\mathbf{k}'\lambda'\hat{n},\mathbf{k}\lambda n_q}|^2$ and $\delta_{n',n-1}\delta_{\mathbf{k}'-\mathbf{k}-\mathbf{q}}$ and $\delta_{n',n+1}\delta_{\mathbf{k}'-\mathbf{k}+\mathbf{q}}$ choose the non-diagonal elements of $|V_{\mathbf{k}'\lambda'\hat{n},\mathbf{k}\lambda n_q}|^2$, so one can easily obtain

$$|V_{\mathbf{k}'\lambda'\hat{n},\mathbf{k}\lambda n}|^2 = | \langle \mathbf{k}'\lambda'n' | \hat{H}_{el-ph} | \mathbf{k}\lambda n \rangle |^2 + |V_{\mathbf{k}'\lambda'\hat{n},\mathbf{k}\lambda n}|^2, \tag{20}$$

and accordingly

$$W_{\mathbf{k}'\lambda'\hat{n},\mathbf{k}\lambda n} = W_{\mathbf{k}'\lambda'\hat{n},\mathbf{k}\lambda n}^{(1)} + W_{\mathbf{k}'\lambda'\hat{n},\mathbf{k}\lambda n}^{(2)} + W_{\mathbf{k}'\lambda'\hat{n},\mathbf{k}\lambda n}^{(3)}, \tag{21}$$

where $W_{\mathbf{k}'\lambda'n,\mathbf{k}\lambda n}^{(1)}$ is due to impurity potential,

$$W_{\mathbf{k}'\lambda'n,\mathbf{k}\lambda n}^{(1)} = \begin{pmatrix} 0 & J^2 \\ J^2 & 0 \end{pmatrix} n_i \delta_{n',n} \delta_{\mathbf{k}',\mathbf{k}}. \tag{22}$$

where n_i is the density of impurities. $W_{\mathbf{k}'\lambda'n,\mathbf{k}\lambda n}^{(2)}$ and $W_{\mathbf{k}'\lambda'n,\mathbf{k}\lambda n}^{(3)}$ are due to electron-phonon Hamiltonian, which $W_{\mathbf{k}'\lambda'n,\mathbf{k}\lambda n}^{(2)}$ represents the phonon absorption,

$$W_{\mathbf{k}'\lambda'n,\mathbf{k}\lambda n}^{(2)} = \delta_{n',n-1} \delta_{\mathbf{k}',\mathbf{k}-\mathbf{q}} \delta_{\lambda',\lambda} \begin{pmatrix} c_q \sqrt{n} & 0 \\ 0 & c_q \sqrt{n} \end{pmatrix}, \tag{23}$$

and $W_{\mathbf{k}'\lambda'n,\mathbf{k}\lambda n}^{(3)}$ corresponds to phonon emission,

$$W_{\mathbf{k}'\lambda'n,\mathbf{k}\lambda n}^{(3)} = \delta_{n',n+1} \delta_{\mathbf{k}',\mathbf{k}+\mathbf{q}} \delta_{\lambda',\lambda} \begin{pmatrix} c_q^* \sqrt{n+1} & 0 \\ 0 & c_q^* \sqrt{n+1} \end{pmatrix}. \tag{24}$$

The deviation of the distribution function from equilibrium state is given by [10]

$$\delta f_\lambda = e \frac{\partial f_0(\epsilon_{\mathbf{k}\lambda})}{\partial \epsilon_{\mathbf{k}\lambda}} \tau_{\mathbf{k}\mathbf{q}\lambda}(\mathbf{E}, \mathbf{v}_{\mathbf{k}\lambda}). \tag{25}$$

where $\mathbf{v}_{\mathbf{k}\lambda} = \frac{1}{\hbar} \nabla_{\mathbf{k}} \epsilon_{\mathbf{k}\lambda}$ is the velocity of conduction electrons, and e_z is a unit vector directed along the normal of the two-dimensional plane, $\delta f_\lambda = f_\lambda - f_0$. Meanwhile $\tau_{\mathbf{k}\mathbf{q}\lambda}$ is defined as follows:

$$\begin{aligned} \frac{1}{\tau_{\mathbf{k}\mathbf{q}\lambda}} &= \sum_{\mathbf{k}',\lambda'} W_{\mathbf{k}'\lambda'n\hat{q},\mathbf{k}\lambda n_q}^{(1)} \left\{ 1 - \frac{|\mathbf{v}_{\mathbf{k}'\lambda'}|}{|\mathbf{v}_{\mathbf{k}\lambda}|} \cos[\theta(\mathbf{v}_{\mathbf{k}\lambda} \wedge \mathbf{v}_{\mathbf{k}'\lambda'})] \right\} \delta(\epsilon_{\mathbf{k}'\lambda'} - \epsilon_{\mathbf{k}\lambda}) + \\ &\sum_{\mathbf{k}',\lambda'} W_{\mathbf{k}'\lambda'n\hat{q},\mathbf{k}\lambda n_q}^{(2)} \left\{ 1 - \frac{|\mathbf{v}_{\mathbf{k}'\lambda'}|}{|\mathbf{v}_{\mathbf{k}\lambda}|} \cos[\theta(\mathbf{v}_{\mathbf{k}\lambda} \wedge \mathbf{v}_{\mathbf{k}'\lambda'})] \right\} \delta(\epsilon_{\mathbf{k}'\lambda'} - \epsilon_{\mathbf{k}\lambda} - \hbar\omega) + \\ &\sum_{\mathbf{k}',\lambda'} W_{\mathbf{k}'\lambda'n\hat{q},\mathbf{k}\lambda n_q}^{(3)} \left\{ 1 - \frac{|\mathbf{v}_{\mathbf{k}'\lambda'}|}{|\mathbf{v}_{\mathbf{k}\lambda}|} \cos[\theta(\mathbf{v}_{\mathbf{k}\lambda} \wedge \mathbf{v}_{\mathbf{k}'\lambda'})] \right\} \delta(\epsilon_{\mathbf{k}'\lambda'} - \epsilon_{\mathbf{k}\lambda} + \hbar\omega). \end{aligned} \tag{26}$$

that $\theta(\mathbf{v}_{\mathbf{k}\lambda} \wedge \mathbf{v}_{\mathbf{k}'\lambda'})$ denotes the angle between $\mathbf{v}_{\mathbf{k}\lambda}$ and $\mathbf{v}_{\mathbf{k}'\lambda'}$.

The expectation value of the spin current in scattering state is defined by

$$\begin{aligned} J_x^i(\mathbf{k}, \lambda) &= J_x^{i(0)}(\mathbf{k}, \lambda) + \hbar \sum_{\mathbf{k}'\lambda'} Re \left[V_{\mathbf{k}'\lambda'n,\mathbf{k}\lambda n} < J_x^i >_{\mathbf{k}'\lambda'n,\mathbf{k}\lambda n} Pr \frac{1}{\epsilon_{\mathbf{k}\lambda} - \epsilon_{\mathbf{k}'\lambda'}} \right. \\ &\left. - V_{\mathbf{k}'\lambda'n,\mathbf{k}\lambda n} < J_x^i >_{\mathbf{k}'\lambda'n,\mathbf{k}\lambda n} i\pi \delta(\epsilon_{\mathbf{k}\lambda} - \epsilon_{\mathbf{k}'\lambda'}) \right]. \end{aligned} \tag{27}$$

The transport spin current in x direction with spin along the x and y axes will be given by

$$J_x^i = \sum_{\mathbf{k}, \mathbf{q}, \lambda} \hat{J}_x^i(\mathbf{k}, \lambda) \delta f_\lambda(\mathbf{k}, \mathbf{q}), \quad (i = x, y) \quad (28)$$

where $\hat{J}_x^i = \frac{\hbar}{2} \{\sigma_i, \hat{v}_x\}$ is the spin current operator and $\hat{v}_x = \hbar^{-1} (\frac{\partial \hat{H}}{\partial k_x})$ is the velocity operator.

The spin-transfer torque is defined as a time derivative of the spin moment and one can obtain this quantity of interest using by its operator defined as

$$\hat{\tau}_\alpha(\mathbf{k}, \lambda) = -i[\hat{\sigma}_\alpha, \hat{H}], \quad (29)$$

$$\tau_\alpha = \sum_{\mathbf{k}, \mathbf{q}, \lambda} \hat{\tau}_\alpha(\mathbf{k}, \lambda) \delta f_\lambda(\mathbf{k}, \mathbf{q}), \quad (\alpha = x, y) \quad (30)$$

3 Results

Our study has been performed on a two-dimensional electron gas system in the presence of spin–orbit couplings and electron–phonon interaction. By utilizing the semiclassical approach, we have calculated the spin accumulation, spin torque, and spin current in the non-equilibrium regime.

In this paper, the electric field is assumed to be applied in x direction and the typical parameters have been considered to be $\epsilon_f = 10eV$, $J = 0.1eV$, $n_i = 10^{16}cm^{-2}$ and $T = 1K$. In addition, Rashba and Dresselhaus spin–orbit couplings have been denoted by $\epsilon_\alpha = m\alpha^2/\hbar^2$, $\epsilon_\beta = m\beta^2/\hbar^2$, respectively.

In the field of information transfer technologies, charge-current could be replaced with spin current that results in improved energy efficiency [16, 17].

As shown in Figs. 1 and 2, optical phonons mediate the non-equilibrium spin current in the presence of the spin–orbit couplings and magnetic impurities. These figures clearly show that the sign and the magnitude of the spin current can be controlled by the SOC's in which the magnitude of spin current components decreases for high ϵ_β or ϵ_α . First the spin current changes rapidly at low lattice vibrations and then, by increasing the D_{opt} , reaches a constant value. Comparing Fig. 1 with Fig. 2 demonstrates that for a same value of ϵ_α and ϵ_β , different spin current components do not have similar behavior even when the given parameters are identical. Forgoing results have shown that in the presence of electron–phonon interaction, both components of the spin current could take non-zero values. Therefore, details of the scattering potential are very important in the generation of the spin current. As reported in Ref. [10], Rashba and Dresselhaus couplings in the presence of the short-range delta function impurity cannot be responsible for the non-equilibrium spin current. It should be noted that the numerical results have indicated that the spin current vanishes in the limit of $D_{opt} \rightarrow 0$ (is not shown in these figures). In the case of non-magnetic impurities, $J = 0$, and for $D_{opt} = 0$, the spin current identically vanishes, which is in agreement with the results in Ref. [10].

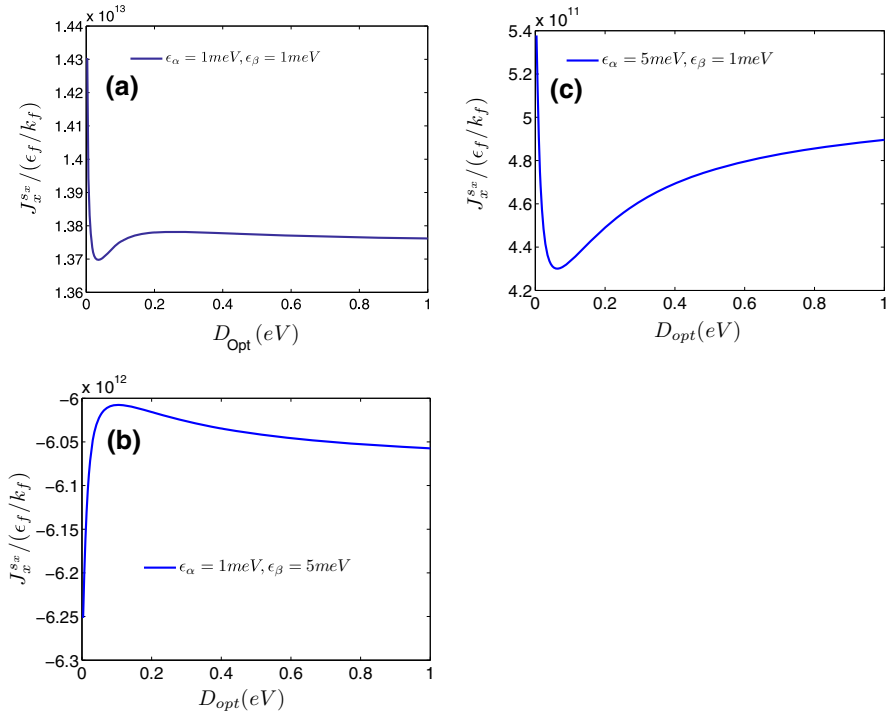


Fig. 1 Longitudinal spin current as a function of the deformation potential for different SO couplings (Color figure online)

Different spin accumulation components have been depicted as a function of the deformation potential in Figs. 3 and 4. In the intermediate range of the optical deformation potential, the momentum of the electrons would be randomized by the electron–phonon interaction. Therefore, by increment of the electron–phonon coupling, spin currents and spin accumulations of the system are reduced to approximately constant values.

As illustrated in these figures, the behavior of the spin accumulation with respect to the electron–phonon interaction can be determined by the spin–orbit couplings.

The influence of the impurities has been considered to provide a realistic system with a typical density of impurities. Fig. 5 shows the spin current components as a function of the deformation potential for $n_i = 10^{10} \text{ cm}^{-2}$, $\epsilon_\alpha = 1 \text{ meV}$, $\epsilon_\beta = 1 \text{ meV}$.

Therefore, in addition to the electron–phonon interaction, that plays a key role in obtaining the spin current, the density of impurities is also important for the spin current values (Figs. 6, 7).

The important results which can be inferred from the Figs. 1, 2, 3, 4 and 5 could be listed as follows: The magnitudes of the spin current and spin accumulation decrease at high Dresselhaus coupling strength. In addition, the Rashba interaction controls both magnitude and the sign of the spin current and spin accumulation. On the other hand, the magnetic configuration of the system has also a dominant contribution in

Fig. 2 Transverse spin current as a function of the deformation potential for different SO couplings (Color figure online)

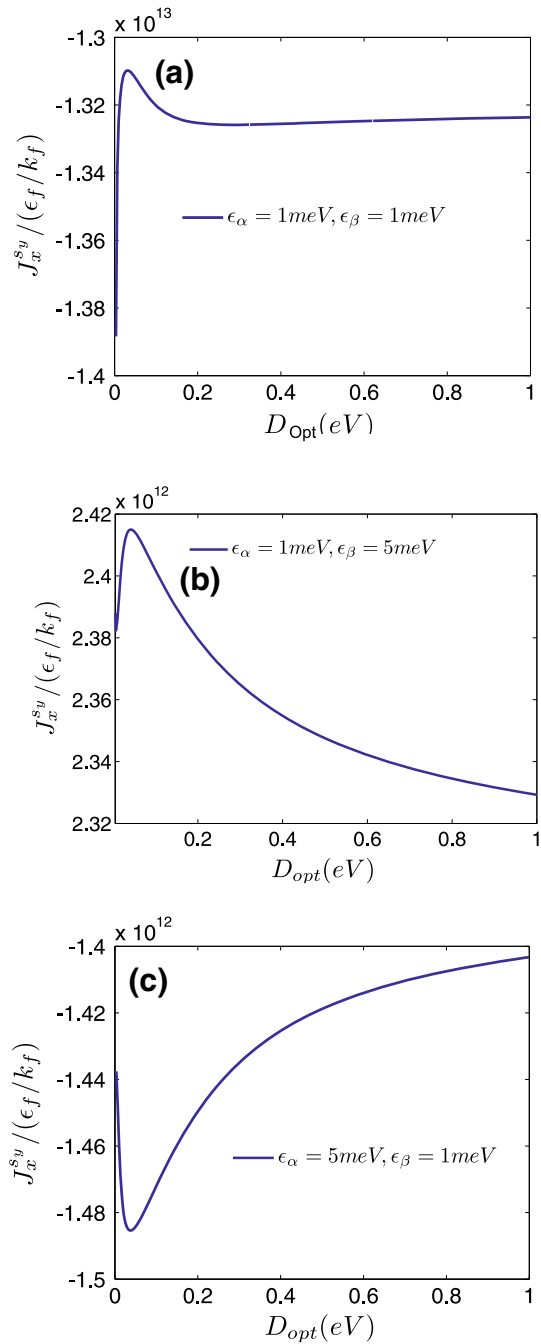


Fig. 3 Longitudinal spin accumulation as a function of the deformation potential for different SO couplings (Color figure online)

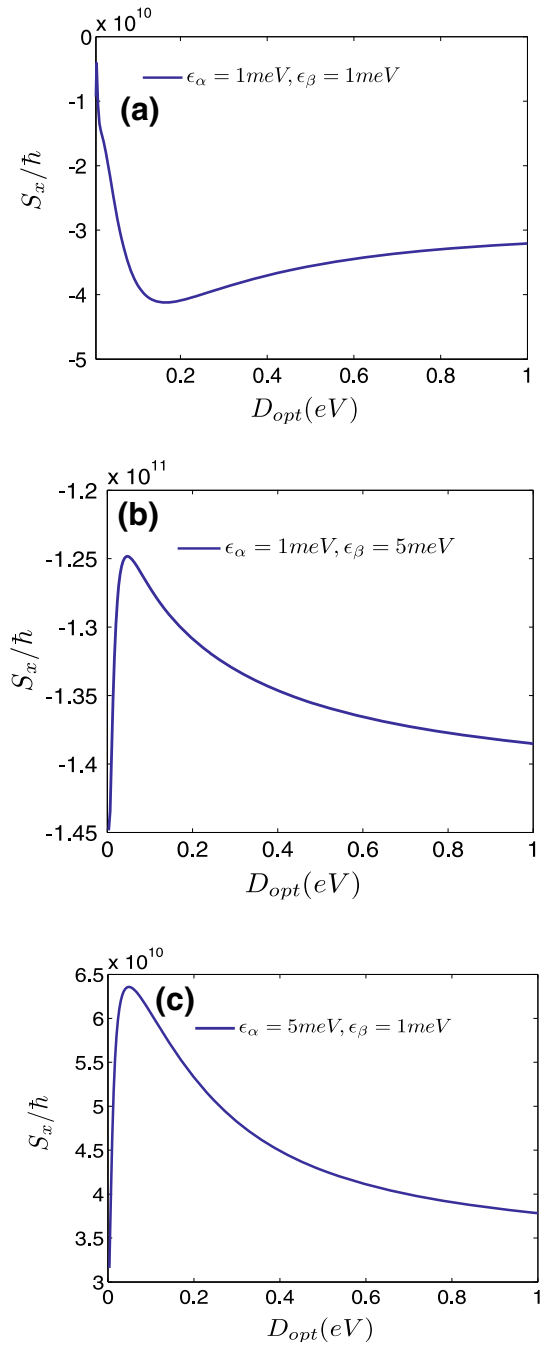
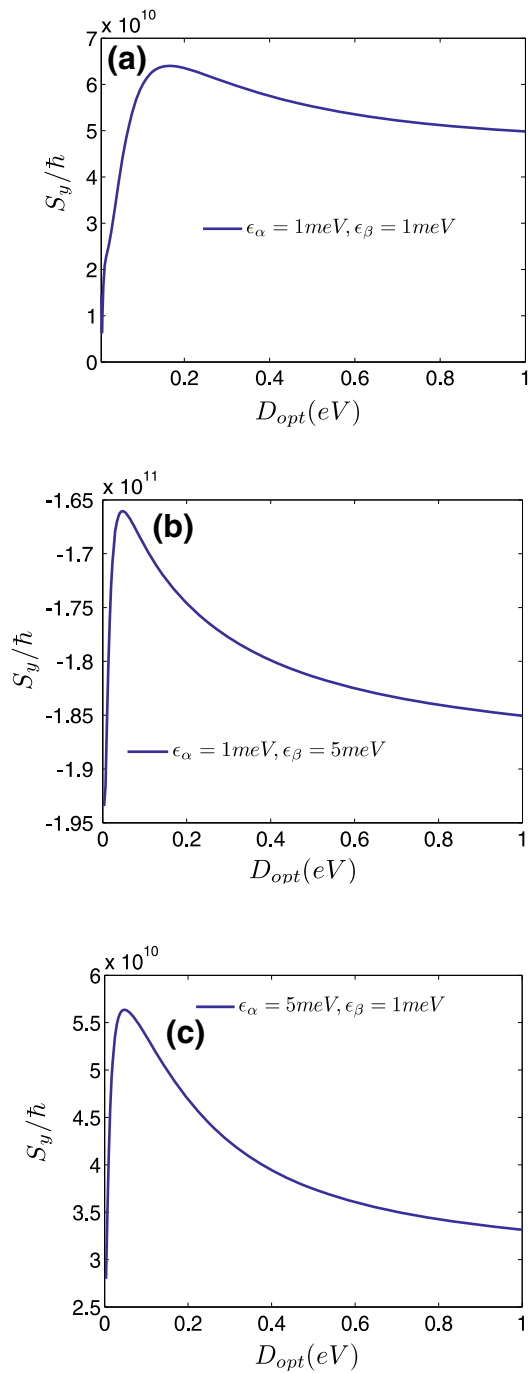


Fig. 4 Transverse spin accumulation as a function of the deformation potential for different SO couplings (Color figure online)



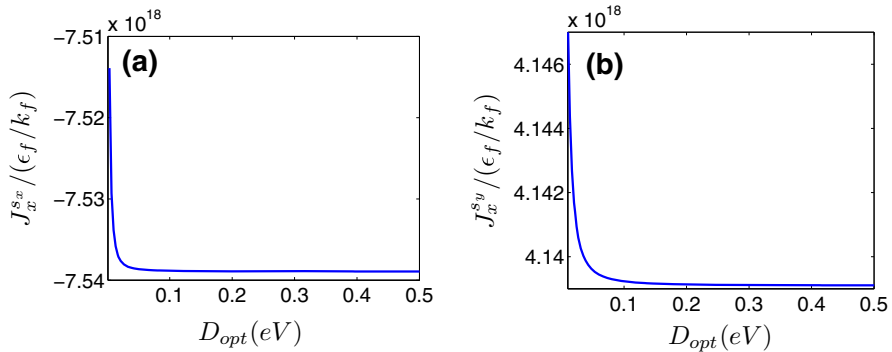


Fig. 5 Transverse and longitudinal spin currents as a function of the deformation potential for $n_i = 10^{10} \text{cm}^{-2}$, $\epsilon_\alpha = 1 \text{meV}$, $\epsilon_\beta = 1 \text{meV}$ (Color figure online)

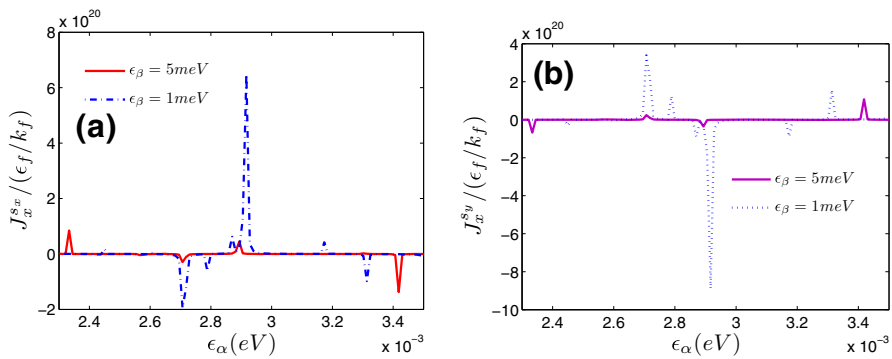


Fig. 6 **a** Longitudinal and **b** transverse spin current as a function of the Rashba SO for different Dresselhaus SO couplings for $D_{opt} = 50 \text{meV}$ (Color figure online)

the transport process. Both the Rashba and Dresselhaus SOIs act like a momentum-dependent effective magnetic fields, the directions of which are different from each other. When $\beta \neq 0$ in the presence of an external electric field (e.g., in the x direction) $\langle H_R \rangle \neq 0$ and $\langle H_D \rangle \neq 0$, non-equilibrium spin density results. Since $\langle k_x \rangle \gg \langle k_y \rangle$, so the average effective magnetic field due to Rashba spin-orbit coupling will tend to be in y direction $\langle H_R \rangle = \langle \alpha(k_y \hat{e}_x - k_x \hat{e}_y) \rangle \simeq -\alpha \langle k_x \rangle \hat{e}_y$ but the average effective magnetic field due to Dresselhaus spin-orbit coupling will tend to be in x direction $\langle H_D \rangle = \langle \beta(k_x \hat{e}_x - k_y \hat{e}_y) \rangle \simeq -\beta \langle k_x \rangle \hat{e}_x$. The total effective magnetic field that the conduction electrons feel is the sum of the two average effective fields, $\langle H_R \rangle$ and $\langle H_D \rangle$; therefore, this direction depends strongly on the relative strength of the spin-orbit couplings.

Finally, we discuss the spin transfer torque components as function of the deformation potential (Figs. 8 and 9). A decrease in the SO couplings leads to a significant change of the spin torque. These spin-orbit couplings can also control the sign of the transverse spin torque.

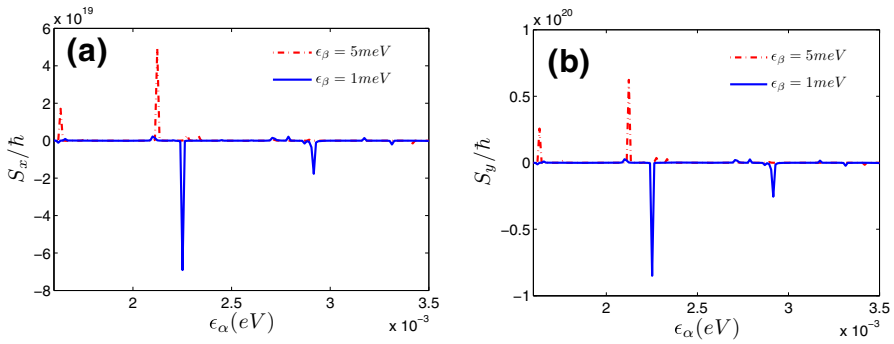


Fig. 7 **a** Longitudinal and **b** transverse spin current as a function of the Rashba SO for different Dresselhaus SO couplings for $D_{opt} = 50\text{meV}$ (Color figure online)

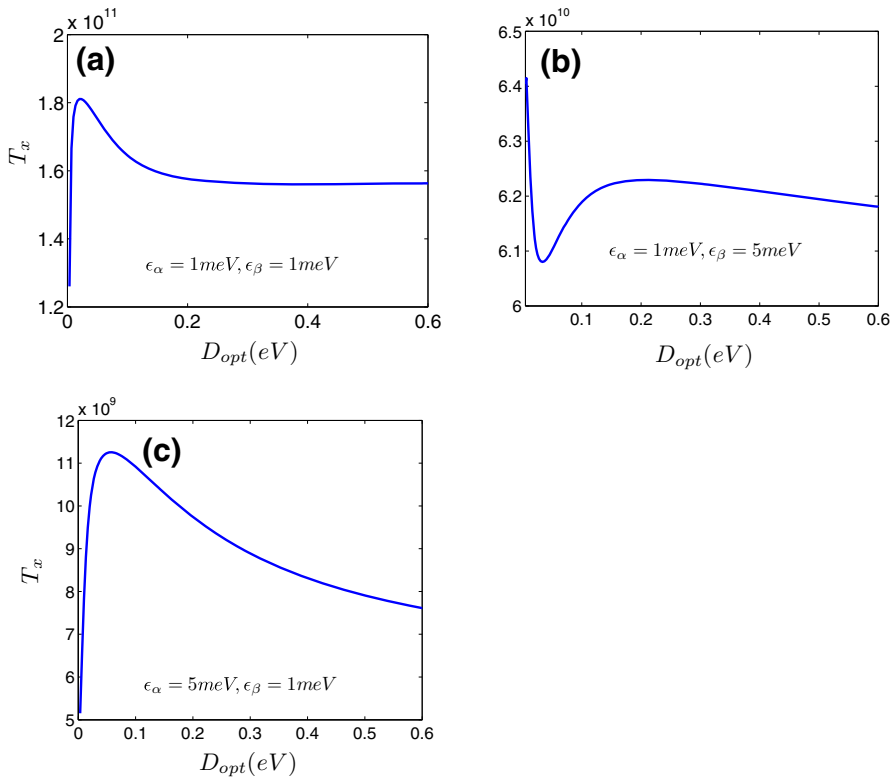


Fig. 8 longitudinal spin torque as a function of the deformation potential for different SO couplings (Color figure online)

Figure 10 shows the spin torque in x and y directions as a function of the Rashba coupling. The differences between these curves clearly demonstrate the importance of the spin–orbit couplings.

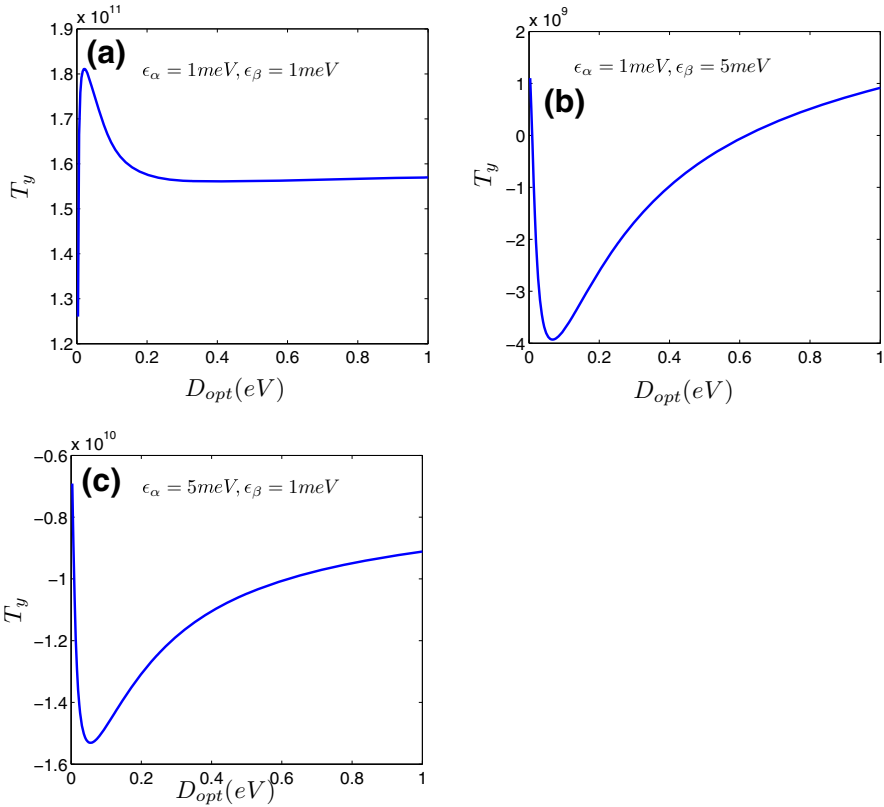


Fig. 9 Transverse spin torque as a function of the deformation potential for different SO couplings (Color figure online)

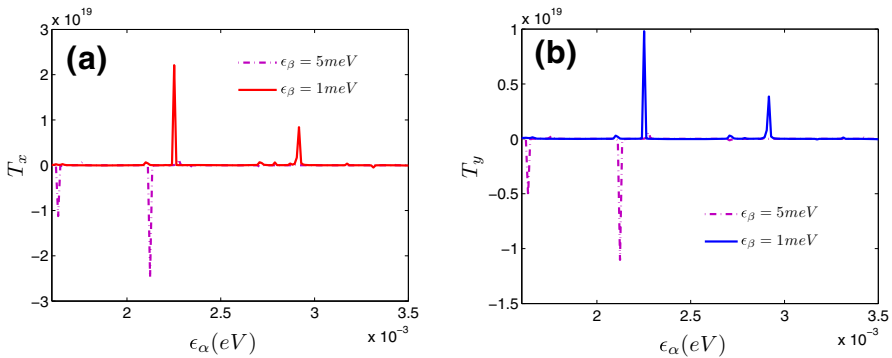


Fig. 10 **a** Longitudinal and **b** transverse spin torque as a function of the Rashba SO for different Dresselhaus SO couplings for $D_{opt} = 50\text{meV}$ (Color figure online)

Spin–orbit couplings can change the band shape and the population of a given state, so these interactions can effectively control the spin-transport parameters. Electron–phonon coupling can also modulate the scattering if the both of the initial and final states be in the same spin-band.

The critical point in our results is the generation of the spin current by the Rashba spin–orbit interaction. Since we can change the Rashba coupling by the gate voltage, we can easily control the spin current of a two-dimensional electron gas in the presence of electron–phonon coupling.

4 Conclusion

In this paper, a semiclassical method by using the Boltzmann approach has been employed for studying the spin-related transport effects in a two-dimensional electron gas system. The results have shown that the electron–phonon coupling plays an important role in generating the non-equilibrium spin current because it was shown that in the absence of the lattice vibrations, Rashba and Dresselhaus SOIs cannot be responsible for the non-equilibrium spin current. It was also demonstrated that even at low electron–phonon coupling, the lattice vibrations have important effects in the spin-transport process modulated by SOIs.

Acknowledgments This research has been supported by the Azarbaijan Shahid Madani university.

References

1. S.A. Wolf, *Science* **294**, 1488 (2001)
2. T. Biswas, T. Kanti, Ghosh. *J. Phys.: Condens. Matter* **25**, 035301 (2013)
3. S. Datta, B. Das, *J. Appl. Phys. Lett.* **56**, 665 (1990)
4. E.I. Rashba, *Solid State Phys.* **2**, 1109 (1960)
5. Y.B. Lyanda-Geller, A.D. Mirlin, *Phys. Rev. Lett* **72**, 1894 (1994)
6. S.V. Iordanskii, *JETP Lett.* **60**, 206 (1994)
7. Y. Lyanda-Geller, *Phys. Rev. Lett.* **80**, 4273 (1998)
8. M. Cardon, N.E. Christensen, G. Fasol, *Phys. Rev. B* **38**, 1806 (1988)
9. G. Dresselhaus, *Phys. Rev.* **100**, 580 (1955)
10. Z. Huang, L. Hu, *Phys. Rev. B* **73**, 113312 (2006)
11. J. Inoue, E.W. Gerrit Bauer, W.M. Laurens, *Phys. Rev. B* **67**, 033104 (2003)
12. K. Výborný, A.K. Alexey, J. Sinova, T. Jungwirth, *Phys. Rev. B* **79**, 045427 (2009)
13. J. Schliemann, D. Loss, *Phys. Rev. B* **8**, 165311 (2003)
14. Ch. Hamaguchi, *Basic Semiconductor Physics*, corrected edn. (Springer, Berlin, 2009)
15. E.B. Ramayya, D. Vasileska, S.M. Goodnick, I. Knezevic, *J. Appl. Phys.* **104**, 063711 (2008)
16. S. Maekawa et al., *Spin Current* (Oxford University Press, Oxford, 2012)
17. Y. Kajiwara, *Nature* **464**, 262 (2010)